

Article

Automatic Radar-Based Step Length Measurement in the Home for Older Adults Living with Frailty

Parthipan Siva ^{1,2,*}, Alexander Wong ², Patricia Hewston ^{3,4}, George Ioannidis ^{3,4}, Jonathan Adachi ^{3,4} , Alexander Rabinovich ^{5,6}, Andrea W. Lee ⁷ and Alexandra Papaioannou ^{3,4}

¹ Chirp Inc., Waterloo, ON N2J 4R2, Canada

² Faculty of Engineering, University of Waterloo, Waterloo, ON N2L 3G1, Canada; a28wong@uwaterloo.ca

³ Geras Centre for Aging Research, St. Peter's Hospital, Hamilton Health Sciences, Hamilton, ON L8M 1W9, Canada; hewstonp@hhsc.ca (P.H.); ioannidis@hhsc.ca (G.I.); jd.adachi@sympatico.ca (J.A.); papaioannou@hhsc.ca (A.P.)

⁴ Department of Medicine, McMaster University, Hamilton, ON L8S 4L8, Canada

⁵ Department of Surgery, McMaster University, Hamilton, ON L8S 4L8, Canada

⁶ ArthroBiologix Inc., Hamilton, ON L8L 5G4, Canada

⁷ Hamilton Health Sciences, Hamilton, ON L8N 3Z5, Canada; leeand@hhsc.ca

* Correspondence: parthipan.siva@mychirp.com

Abstract: With an aging population, numerous assistive and monitoring technologies are under development to enable older adults to age in place. To facilitate aging in place, predicting risk factors such as falls and hospitalization and providing early interventions are important. Much of the work on ambient monitoring for risk prediction has centered on gait speed analysis, utilizing privacy-preserving sensors like radar. Despite compelling evidence that monitoring step length in addition to gait speed is crucial for predicting risk, radar-based methods have not explored step length measurement in the home. Furthermore, laboratory experiments on step length measurement using radars are limited to proof-of-concept studies with few healthy subjects. To address this gap, a radar-based step length measurement system for the home is proposed based on detection and tracking using a radar point cloud followed by Doppler speed profiling of the torso to obtain step lengths in the home. The proposed method was evaluated in a clinical environment involving 35 frail older adults to establish its validity. Additionally, the method was assessed in people's homes, with 21 frail older adults who had participated in the clinical assessment. The proposed radar-based step length measurement method was compared to the gold-standard Zeno Walkway Gait Analysis System, revealing a 4.5 cm/8.3% error in a clinical setting. Furthermore, it exhibited excellent reliability (ICC(2,k) = 0.91, 95% CI 0.82 to 0.96) in uncontrolled home settings. The method also proved accurate in uncontrolled home settings, as indicated by a strong consistency (ICC(3,k) = 0.81 (95% CI 0.53 to 0.92)) between home measurements and in-clinic assessments.

Keywords: FMCW radar; mmwave radar; ambient sensing; gait analysis; step length



Citation: Siva, P.; Wong, A.;

Hewston, P.; Ioannidis, G.;

Adachi, J.; Rabinovich, A.;

Lee, A.W.; Papaioannou, A.

Automatic Radar-Based Step Length Measurement in the Home for Older Adults Living with Frailty. *Sensors* **2024**, *24*, 1056. <https://doi.org/10.3390/s24041056>

Academic Editor: Antonio Lázaro

Received: 3 January 2024

Revised: 22 January 2024

Accepted: 2 February 2024

Published: 6 February 2024



Copyright: © 2024 by the authors. Licensee MDPI, Basel, Switzerland. This article is an open access article distributed under the terms and conditions of the Creative Commons Attribution (CC BY) license (<https://creativecommons.org/licenses/by/4.0/>).

1. Introduction

With an aging population, multiple countries are facing challenges caring for older adults. Care facilities are overloaded, and hospitals are becoming overburdened. Consequently, there has been a shift towards adopting aging-in-place strategies aimed at enabling older adults to stay in their homes for as long as possible while receiving homecare support. Aging in the home is a more scalable solution than building care facilities and is also a preferable solution for aging individuals. Studies have shown that monitoring aging older adults and individuals with chronic conditions in the home can have a 500% reduction in cost to the health system [1].

To keep people in the home safely, early detection and prediction of frailty, fall risk, and hospitalization risk are essential to provide timely interventions and reduce emergency

room visits. Gait analysis has been shown to be a predictor of risk factors such as falls, frailty and hospitalization [2–6]. Gait has many parameters such as speed, step length, cadence, etc. While these parameters are not independent, they do have complex relationships. For example, gait speed can be maintained with different step lengths by changing ones cadence.

When someone walks with a shuffling gait—taking shorter steps, keeping their feet closer to the ground, and leaning forward—fall risk is increased. Identifying this walking pattern early (by investigating step length) can help in the early detection of falls. In [7], different gait parameters' importance for predicting frailty was evaluated objectively based on a recursive feature elimination algorithm and ranked with the Gini impurity. Based on the feature importance, step length was concluded to be more important than gait speed in predicting frailty [7]. Furthermore, they note that adding other gait parameters to step length and gait speed created only a slight increase in accuracy. Similarly, [8] found through a multi-variate analysis that gait speed and step length were important for predicting dependency and mortality but for predicting institutionalization step length alone was the better predictor. For fall risk assessment, ref. [9] showed that people with normal gait speed and shorter step length were also at higher risk of falls. Ref. [9] concluded that gait speed and step length contribute additively to the assessment of fall risk.

Building upon the insights gleaned from these studies [4–9], it becomes evident that gait speed and step length play pivotal roles in evaluating frailty, fall risk, and hospitalization risk in older adults. While several methods have been proposed for the continuous monitoring of gait speed in a home environment [10–15], a significant gap exists concerning step length measurement in the home.

This paper aims to address this critical gap by proposing a radar-based approach for monitoring step length within the home setting. Preliminary approaches for step length measurement have been studied in controlled laboratory environments, utilizing cameras [16], light detection and ranging (lidar) [17], and radar [18]. While camera-based methods are intrusive for in-home use and lidar-based approaches are relatively costly, radar-based solutions offer promise as a privacy-preserving and cost-effective means of measuring step length in a home setting. However, radar has been tested only in laboratory settings with young healthy subjects walking 10 m or more directly towards the radar. A long walking sequence is essential to mitigate the impact of acceleration and deceleration, thereby obtaining a more accurate average step length measurement. Walking directly toward the radar enhances the signal-to-noise ratio (SNR) and guarantees that the subject remains within the optimal distance and speed sensitivity range of the radar.

For radar-based step length measurement in a home environment, several challenges must be overcome. First, a means of measuring step length where subjects can walk in any directions is needed. Second, the measurement of step lengths should be conducted during short walks, given the impracticality of expecting 10 m walks within a home environment, where the average room size is smaller than 10 m. Finally, a comprehensive evaluation of radar-based step length measurement using frail older adults is needed to show the validity and reliability of using radar-based step length measurement for health risk assessment.

To tackle the challenges associated with radar-based step length measurement in home settings and to address the absence of step length evaluation involving frail older adults, this paper presents the following contributions:

1. Introduction of the first radar-based step length measurement in an unrestricted home environment by automatically selecting optimal walk sequences within the home to measure step lengths.
2. Provision of a comprehensive evaluation of the proposed in-home step length measurement for both reliability, through test–retest reliability testing, and validity, by correlating with established in-clinic step length measurements. This evaluation is conducted with frail older adults in their own homes over a two-week period.
3. Presentation of a thorough in-clinic validation of step length measurement involving frail older adults undergoing five different types of walks.

These real-world methods and evaluations are crucial to validate the effectiveness of radar-based approaches for continuous in-home gait monitoring of older adults aging in place.

2. Related Works

There is a scarcity of controlled setting studies on radar-based step length measurement, with none conducted in an uncontrolled environment. The existing works, outlined in Table 1, primarily adopt two approaches: one based on Doppler echoes from the ankle/toes [19,20] and the other on Doppler echoes from the torso [18,21–23]. The ankle/toe-based methods, as highlighted in [23], necessitate close proximity of the radar sensor to the walker’s feet, making them applicable only in controlled settings, such as treadmill-based studies. Conversely, the torso-based methods are deemed more suitable for ambient step length measurement in a home setting due to the larger size and density of the torso, resulting in stronger radar echoes compared to the ankles/toes.

Table 1. Existing radar-based step length measurement techniques using trunk movement.

Method	Distance (m)	No. of Participants	Participants	Ground Truth
[21]	4	3	Young adults	Marker attached to shoe
[22]	25.2 [†]	4	Young adults	Fixed 70 cm steps
[18]	56 [‡]	5	Young adults	Fixed 70 cm steps
[23]	10	10	Young adults	MOCAP

[†] 4.2 m back and forth three times; [‡] 14 m back and forth two times.

The torso-based method hinges on the cyclical pattern of torso speed throughout the gait cycle, as depicted in Figure 1. Step length is determined by measuring the distance between torso speed peaks [18,22], the distance between torso acceleration peaks [23], or by dividing the average gait speed by the step frequency. The latter is calculated through frequency decomposition of the torso speed profile [21].

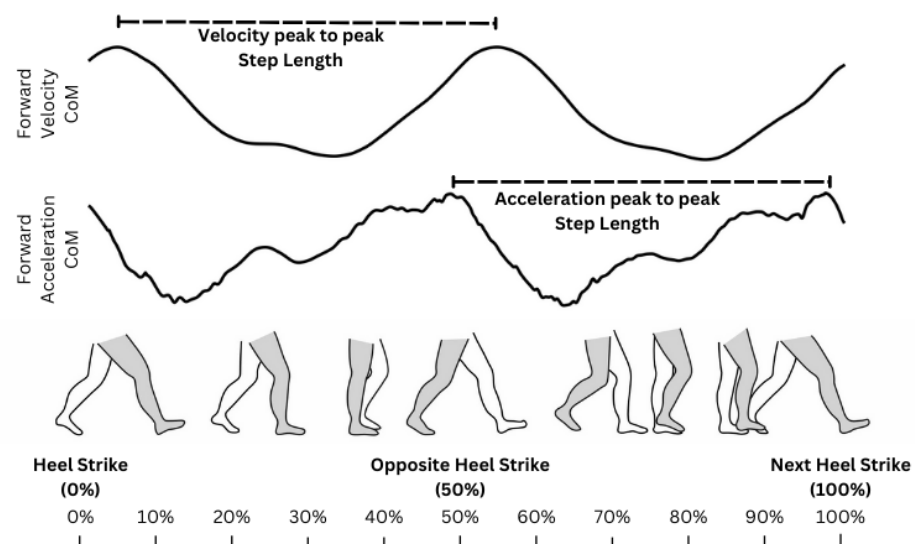


Figure 1. The forward velocity and acceleration of the center of mass during a single gait cycle. The peak-to-peak distance of velocity and acceleration is equivalent to one step length. Illustration based on speed profile and gait descriptions is given in [24,25].

The existing works discussed in Table 1 exhibit several limitations. Firstly, they predominantly focus on evaluating their methodologies using a limited sample of young, healthy individuals without mobility issues, neglecting the assessment of frail older adults who may exhibit deviations from a healthy gait. Secondly, these methodologies presuppose long, constant-speed walk sequences ranging from 4 to 14 m or repeated walks up to 56 m,

which prove impractical in a home setting, particularly for older adults who are frail and incapable of maintaining a constant speed over extended distances. Thirdly, the removal of the initial and final 1–2 m of walk sequences to eliminate acceleration and deceleration effects necessitates even longer walk sequences, thereby excluding the analysis of typical short walks anticipated in a home environment. Lastly, the investigated works do not explore the passive measurement of step length in an unconstrained home environment.

Each individual approach has its own set of limitations. The acceleration peak-to-peak method proposed by [23] involves taking the derivative of the torso speed profile, making it susceptible to noise inherent in the torso speed measurement. The step frequency-based method introduced by [21] relies on maintaining a constant speed during the walk, achieved by eliminating acceleration and deceleration effects at the walk's start and end. However, this method is impractical for home settings where shorter walk sequences prevent effective compensation for acceleration effects. Consequently, in this study, the torso speed peak-to-peak distance method, as utilized in [18,22], is employed for step length measurement.

3. Hardware

In the proposed approach, the Chirp smart sensor CHIRP-01-T [26], affixed to the wall, is employed to monitor individuals, extract torso speeds, and ascertain step length. The Chirp smart sensor is an Internet of Things (IoT) device equipped with onboard processing and utilizes the Texas Instruments (TI) IWR6843AOP radar. The TI radar operates as a frequency-modulated continuous-wave (FMCW) radar within the frequency range of 60–64 GHz. It is approved for use by the Federal Communications Commission (FCC) of the United States [27]. Moreover, studies have confirmed the safety of this radar frequency range for continuous monitoring of humans [28,29].

Due to bandwidth constraints for continuous 24/7 data collection within a home and the limited computational capabilities of the IoT device, only radar point clouds, as detailed in Section 4.1, are processed at a rate of 10 frames per second to track individuals and measure step lengths.

3.1. Clinical Setup

Data collection was conducted in a large multipurpose room within a hospital setting (Figure 2) with a 4 m ProtoKinetics Zeno Walkway (Havertown, PA, USA) at a sampling frequency of 100 Hz. The Chirp device (Waterloo, ON, Canada) was positioned at the end of the walking path at a distance of 6.03 m from the start and 2.03 m from the end of the ProtoKinetics Walkway at a sampling frequency of 10 Hz (10 frames per second). The ProtoKinetics Zeno Walkway (pressure sensors) and Chirp devices (radar positioning) collected data simultaneously.

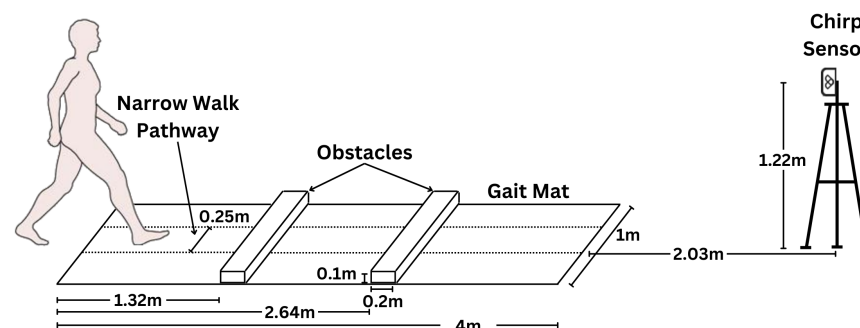


Figure 2. In-clinic setup of the 4 m ProtoKinetics Zeno Walkway Gait Analysis System and Chirp Smart Home Sensor for testing concurrent validity of step length measurement. Obstacles are only used for obstacle walks. Narrow walk pathway is used for narrow walking scenario only.

The clinical data collection for all participants occurred in multiple sessions over a four-month period. All efforts were made to set up the Zeno Walkway and Chirp sensor at the exact locations specified in Figure 2. The location of clutter (tables, chairs, etc.) in the room between sessions could vary. During each session, two to three research assistants were present in the room within the field of view of the radar sensor. Furthermore, for older adults with more severe frailty, a research assistant walked behind the individual during their walk across the Zeno Walkway for safety.

3.2. Home Setup

For in-home step length measurement, participants were directed to install Chirp sensors in their bedroom, living room, and kitchen. Guidelines were provided to position the Chirp sensor between 121 cm (48 inches) and 132 cm (52 inches) above the floor, which corresponds to the typical height of residential wall switches (see Figure 3a). Participants were further instructed to place the Chirp sensor as centrally as possible on the wall, ensuring full coverage of the room (see Figure 3b). Following installation, participants utilized the Chirp Labs App to connect the Chirp sensor to their WiFi and assigned the names bedroom, kitchen, and living room to each respective sensor.

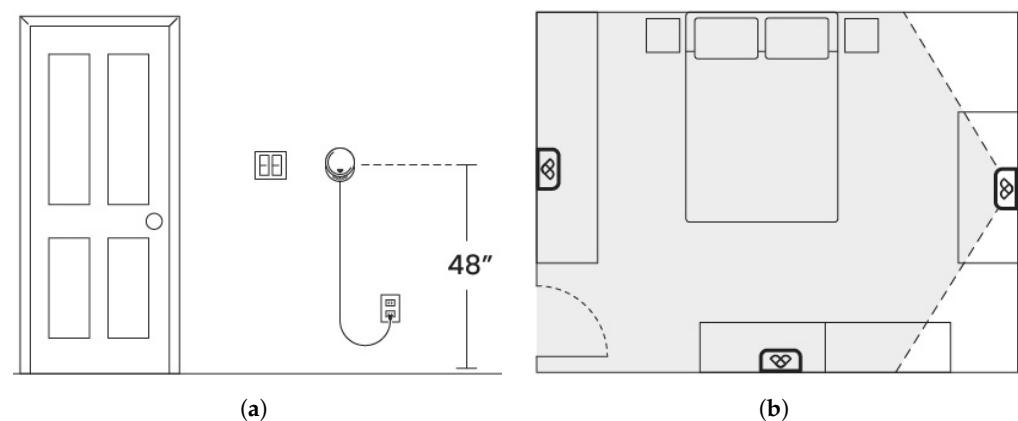


Figure 3. Placement of Chirp sensor in the room. (a) Elevation at switch height. (b) Possible locations of the Chirp sensor at center of wall covering entire room.

For inter-device test–retest reliability within the home between week 1 and week 2, participants were requested to remount all Chirp sensor devices after the first week of data collection (e.g., relocating the kitchen device to the bedroom, the bedroom device to the living room, and the living room device to the kitchen).

The installation and setup process was left to the discretion of the user, and the authors did not modify or validate the device placement. Consequently, the placement reflects how families might set up the devices in a consumer setting.

4. Proposed Approach

The overall approach for step length measurement in a home setting and clinical setting is illustrated in Figure 4. The TI signal processing software development kit (SDK) [30] is used to produce radar point clouds at 10 frames per second (FPS). The point clouds are used to detect and track individuals moving in the scene as outlined in [31]. A novel track filtering method is presented in this paper to identify tracks that can be used for step length measurement in the home or in the clinical setting. Once viable tracks are identified, a novel outlier rejection-based torso speed analysis is presented to measure the average step length.

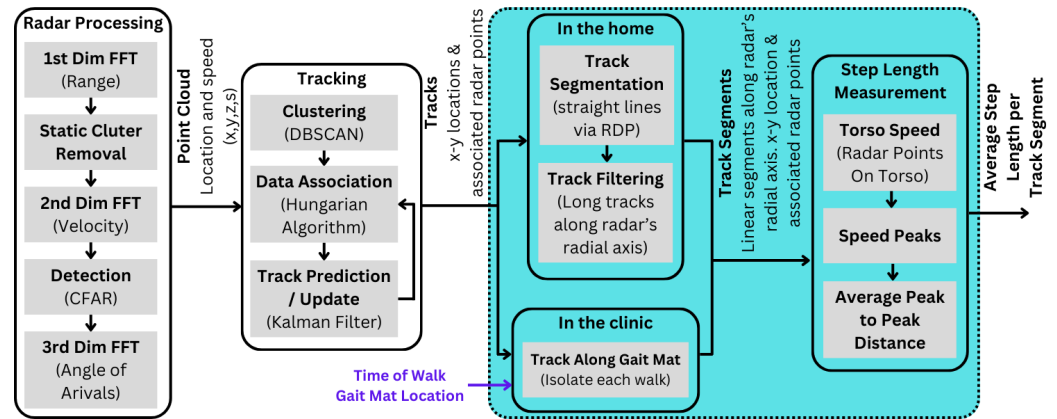


Figure 4. Step length measurement methodology: Radar signal processing generates 3D point clouds with speeds, enabling detection and tracking of individuals. In the home, linear track segments along the radar’s radial axis are isolated, while in the clinic, track segments along Zeno Walkway’s linear path are extracted. Step length is determined as the peak-to-peak distance of torso speed. The contributions of this paper are highlighted by the dashed rectangle (cyan).

4.1. Radar Point Cloud

The Texas Instruments radar processing tool chain [30] consisting of signal processing, static clutter removal, and constant false alarm rate (CFAR) detection is used to obtain a radar point cloud at time t . The point cloud is formed by a set of moving points detected by the radar (Figure 5a), where each point consists of a location and speed.

$$\mathcal{P}_t = \{p_t^1, \dots, p_t^i, \dots, p_t^n\} \quad (1)$$

where t is the current time, and the i^{th} point is $p_t^i = (x_i, y_i, z_i, s_i)$. Location x, y, z is in meters, and speed s is in meters per second.

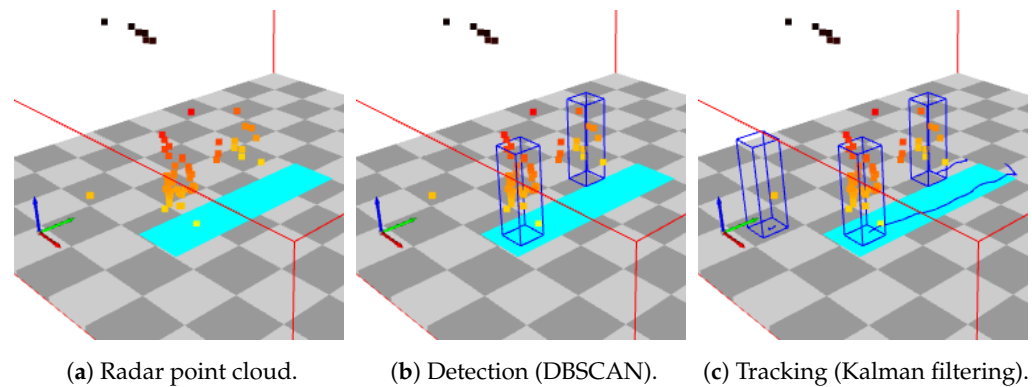


Figure 5. Tracking illustration: Radar point clouds are clustered to form detections, which are associated to tracks through the Hungarian algorithm and tracked using Kalman filtering. The floor is depicted with a 1 m by 1 m checkerboard pattern, while Zeno Walkway is represented by a cyan rectangle. The blue rectangular prism represents observations of people or tracked location of people.

4.2. Detection and Tracking

Using the radar point cloud \mathcal{P}_t , a detection and tracking approach based on DBSCAN clustering for detection (Figure 5b), data association via Hungarian assignment and Kalman filtering for tracking (Figure 5c) as outlined in [31] is used for tracking people in the scene. This results in a set of tracks:

$$\mathcal{T} = \{T_1, \dots, T_i, \dots, T_N\} \quad (2)$$

Each track is defined as

$$T_i = \{(x_{t_0}, y_{t_0}, \mathcal{S}_{t_0}), \dots, (x_{t_j}, y_{t_j}, \mathcal{S}_{t_j}), \dots, (x_{t_N}, y_{t_N}, \mathcal{S}_{t_N})\} \quad (3)$$

where $\mathcal{S}_{t_j} \subseteq \mathcal{P}_{t_j}$ (\mathcal{P} is defined in (1)) and (x_{t_j}, y_{t_j}) is the track location in the room at time t_j . As in [31], we track moving objects' location only in the $x - y$ plane, ignoring elevation z . \mathcal{S}_{t_j} is formed by DBSCAN clustering from radar point cloud \mathcal{P}_{t_j} at time t_j and assigned to track T_i during data association via Hungarian assignment.

4.3. Tracks in the Clinic

In the clinic, the radar is set up in front of a Zeno Walkway (Figure 2). For fair comparison, radar-based step length measurement must be conducted over the track segment starting and ending on the Zeno Walkway. The clinic setting is reproduced for each participant such that the Zeno Walkway starts and ends at the coordinates $g_s = (0, 6.03)$ and $g_e = (0, 2.03)$, respectively. Furthermore, for each walk by participant i , a start time t_i^w and Zeno Walkway average step length g_i^w was recorded.

Given all the tracks \mathcal{T} (defined in (2)) obtained during participant testing, the track segment associated with the in-clinic walks are

$$\mathcal{L}' = \{L_1^1, L_1^2, \dots, L_1^W, \dots, L_i^k, \dots, L_P^W\} \quad (4)$$

where P is the number of participants, and W is the number of walks for each participant. The track segment L_i^k is obtained as the track segment starting near g_s and ending near g_e and is closest in starting time to t_i^w .

4.4. Tracks in the Home

The Doppler radar is most sensitive to speed changes along the radial axis. As a result, the best way to isolate small fluctuations in torso speed, which are caused during the normal gait cycle, is to look at the torso speed when a person is traveling along the radial axis of the radar. To this end, given all the tracks \mathcal{T} from a home setting, the track segments that are in a relatively straight line going along the radial axis is isolated for step length measurement. First, all tracks are segmented into linear segments (Section 4.4.1), and then the linear segments are classified as valid segments traveling along the radar's radial axis (Section 4.4.2).

4.4.1. Track Segmentation

To isolate instances where individuals are walking towards or away from the radar (i.e., along the radar's radial axis), we segment all tracks into linear segments. The $x - y$ locations of the track T_i are treated as a polyline, which is decimated using the Ramer–Douglas–Peucker (RDP) algorithm [32]. The RDP algorithm has a single parameter ϵ that controls the decimation and is the maximal distance allowed between a point on the polyline and the linear representation of that polyline.

The points selected by the RDP decimation are used to segment the track T_i into linear track segments. If the RDP algorithms select $M_i + 1$ points along track T_i to keep, then track T_i will be segmented into M_i linear segments as illustrated in Figure 6. We represent the linear segments as f

$$T_i = \{L_i^1, \dots, L_i^k, \dots, L_i^{M_i}\} \quad (5)$$

The set of all linear track segments becomes:

$$\mathcal{L} = \{L_1^1, \dots, L_1^{M_1}, \dots, L_i^1, \dots, L_i^k, \dots, L_i^{M_i}, \dots, L_N^{M_N}\} \quad (6)$$

where N is the number of tracks as defined in (2), M_i is the number of linear segments in track i and the cardinality of the set, $|\mathcal{L}| = \sum_{i=1}^N M_i = m$, is the number of linear track segments from the home.

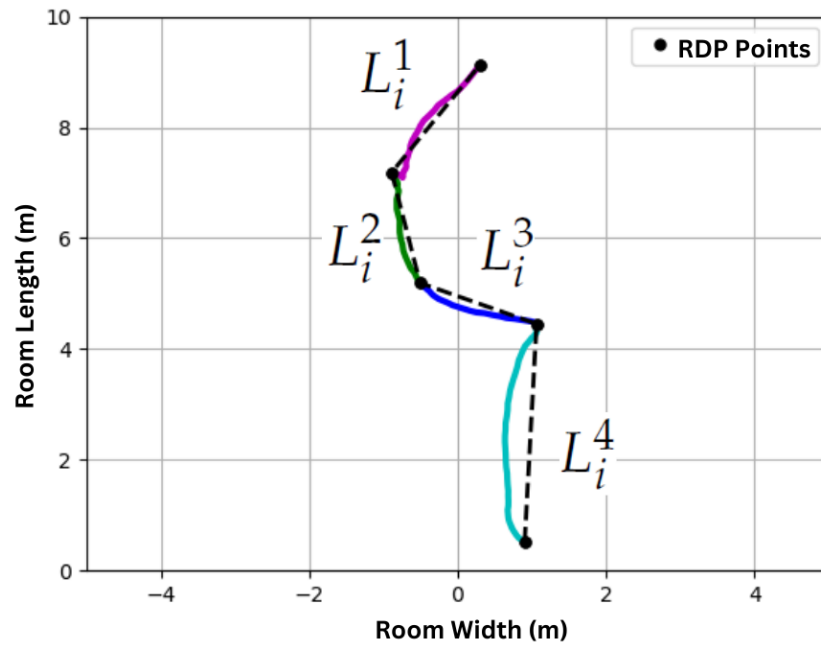


Figure 6. Track T_i is segmented into linear track segments L_i^1, \dots, L_i^4 using the Ramer–Douglas–Peucker algorithm. $\varepsilon = 0.5$ m for this figure. The segments of track T_i corresponding to L_i^1, L_i^2, L_i^3 , and L_i^4 are indicated by the colors magenta, red, blue and cyan respectively.

4.4.2. Track Filtering

Given linear track segments, the segments along the radial axis of the radar must be isolated. Because of the radar's sensitivity along the radial axis, the robust way to measure instantaneous changes in torso speeds is in the radial direction. To this end, given a linear track segment

$$L_i^k = \{(x_{t_0}, y_{t_0}, \mathcal{S}_{t_0}), \dots, (x_{t_j}, y_{t_j}, \mathcal{S}_{t_j}), \dots, (x_{t_N}, y_{t_N}, \mathcal{S}_{t_N})\} \quad (7)$$

we define

$$r_{t_0} = \sqrt{(x_{t_0})^2 + (y_{t_0})^2} \quad (8)$$

$$r_{t_N} = \sqrt{(x_{t_N})^2 + (y_{t_N})^2} \quad (9)$$

$$d_i^k = \sqrt{(x_{t_0} - x_{t_N})^2 + (y_{t_0} - y_{t_N})^2} \quad (10)$$

$$\theta_i^k = \arccos \left(\frac{(\max(r_{t_0}, r_{t_N}))^2 + (d_i^k)^2 - (\min(r_{t_0}, r_{t_N}))^2}{2d_i^k \max(r_{t_0}, r_{t_N})} \right) \quad (11)$$

As illustrated in Figure 7, θ_i^k is the rotation angle needed about the radially furthest track endpoint to rotate the track directly towards (away from) the radar. The classification of track segment L_i^k is

$$c_i^k = \begin{cases} 1 & \text{if } d_i^k \geq D \text{ and } \theta_i^k \leq \gamma \\ 0 & \text{otherwise} \end{cases} \quad (12)$$

where $c_i^k = 1$ indicates valid linear tracks segment along radar's radial axis that is sufficiently long enough to detect step lengths and its relative orientation to radar's radial axis is small.

This results in a set of valid radially aligned linear track segments:

$$\mathcal{L}' = \{L_i^k \in \mathcal{L} : c_i^k = 1\} \quad (13)$$

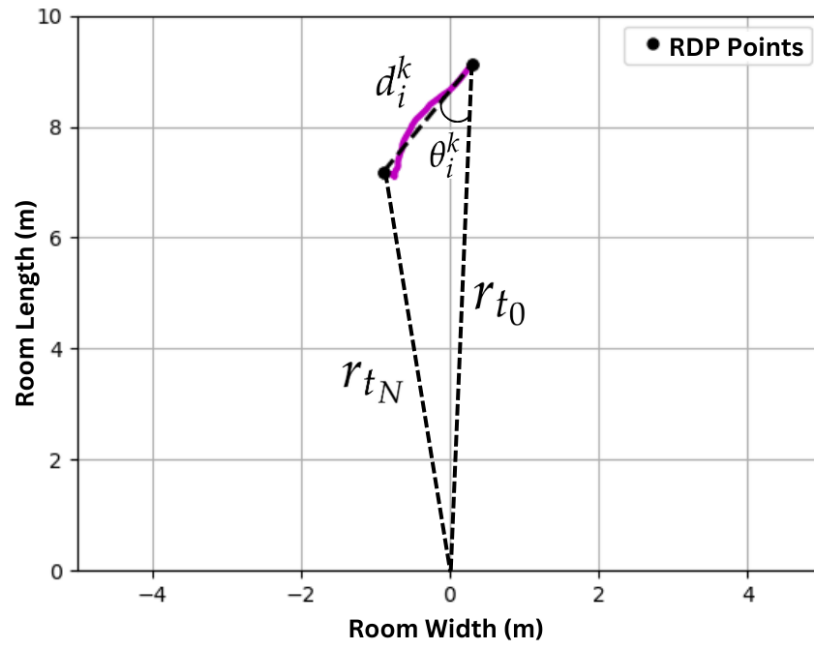


Figure 7. Linear track segment L_i^k has a length d_i^k (10) and an orientation θ_i^k (11) that is needed to orient the track along radar's radial axis.

4.5. Step Length Measurement

Given a linear track segment along radar's radial axis, $L_i^k \in \mathcal{L}'$, from the home (13) or at the clinic (4), the average step length needs to be measured. Similar to [18,22], step length measurement is obtained as the peak-to-peak distance of the torso speed.

4.5.1. Torso Speed

Each linear track segment $L_i^k \in \mathcal{L}'$ has a set of tracked locations:

$$L_i^k = \{(x_{t_0}, y_{t_0}, \mathcal{S}_{t_0}), \dots, (x_{t_j}, y_{t_j}, \mathcal{S}_{t_j}), \dots, (x_{t_N}, y_{t_N}, \mathcal{S}_{t_N})\} \quad (14)$$

where

$$\mathcal{S}_{t_j} = \{(x_1, y_1, z_1, s_1), \dots, (x_a, y_a, z_a, s_a), \dots, (x_N, y_N, z_N, s_N)\} \quad (15)$$

represents the set of radar points on the person being tracked, which includes points on the torso, arms, legs, etc. From this, points on the torso $\mathcal{S}_{t_j}^{torso} \in \mathcal{S}_{t_j}$ are isolated based on elevation data and direction of travel.

The radar is placed 121 cm (48 inches) to 132 cm (52 inches) above the floor, as such we conservatively estimate torso points to be in the range $-Z_{torso} \leq z_a \leq Z_{torso}$. Furthermore, if the person is traveling towards the radar, we expect the Doppler speed of the torso to be $-ve$ and if the person is traveling away from the radar, we expect the Doppler speed of the torso to be $+ve$. This distinction is important, because the arms can be traveling in the opposite direction to the torso.

Specifically, given linear track segment L_i^k in (14), the radial distance to the start r_{t_0} (8) and end r_{t_N} (9) locations, the radar points on the torso $\mathcal{S}_{t_j}^{torso} \subseteq \mathcal{S}_{t_j}$ is defined as

$$\mathcal{S}_{t_j}^{torso} = \{(x_a, y_a, z_a, s_a) \in \mathcal{S}_{t_j} : -Z_{torso} \leq z_a \leq Z_{torso} \text{ and } \alpha s_a > 0\} \quad (16)$$

$$\alpha = \begin{cases} -1 & \text{if } r_{t_N} < r_{t_0} \\ +1 & \text{if } r_{t_N} > r_{t_0} \end{cases} \quad (17)$$

The torso speed at each time step t_j is v_{t_j} and is computed as the average of speeds in $\mathcal{S}_{t_j}^{torso}$.

$$v_{t_j} = \frac{\sum_a s_a \in \mathcal{S}_{t_j}^{torso}}{|\mathcal{S}_{t_j}'|} \quad (18)$$

Given a set of torso speed v_{t_j} the linear track segment L_i^k becomes

$$L_i^k = \{(x_{t_0}, y_{t_0}, v_{t_0}), \dots, (x_{t_j}, y_{t_j}, v_{t_j}), \dots, (x_{t_N}, y_{t_N}, v_{t_N})\} \quad (19)$$

where x, y is the location of the person and v is the Doppler torso speed of the person.

Acquiring torso speed from radar points linked to a track offers a benefit. In situations with multiple individuals within the radar field of view, as depicted in Figure 5c, it enables the determination of accurate torso speeds for each person. This enhances the reliability of torso speed estimation, particularly in noisy conditions.

4.5.2. Average Peak-to-Peak Distance

The torso speeds from (19) are used to find peaks as illustrated in Figure 8. Given the torso speeds on the linear track segment, a center surrounded window of 0.4 s (5 points given a 10 FPS) is used for non-maximum suppression (NMS). After NMS, all peaks are found and sorted in descending order of speed. Starting at the fastest speed (highest peak), peaks are kept as valid peak if the peak-to-peak time is at least R seconds. Once all valid peaks are found, the peak-to-peak distance and peak-to-peak time are obtained as potential step length and step time.

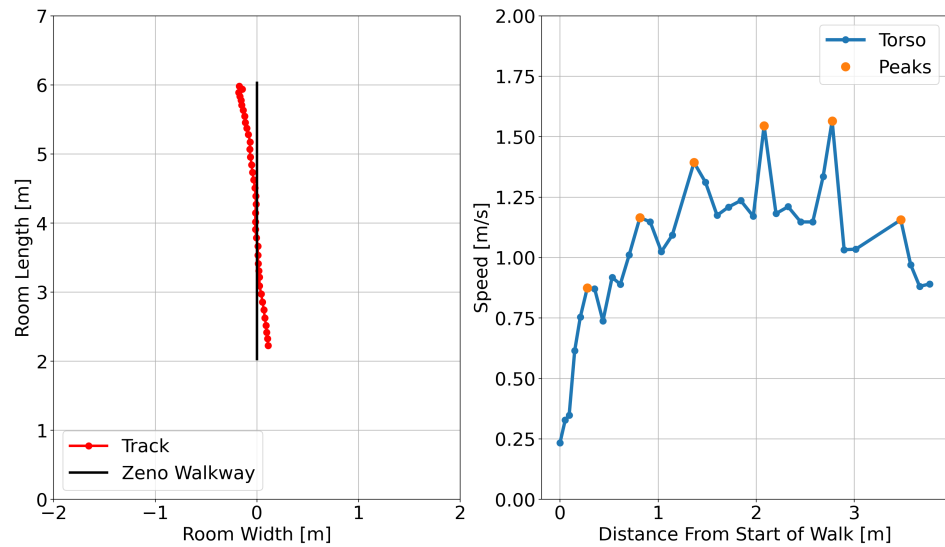


Figure 8. Control (normal speed) walk by a participant: On the left, the tracked location overlaid with the expected location of the Zeno Walkway. On the right, the Doppler torso speed, featuring detected torso speed spikes. Notably, the speed trend is non-constant due to the acceleration and deceleration effects of starting and stopping.

The peak detection algorithm may skip a step due to noise or the irregular gait of frail older adults, leading to inaccuracies in measuring peak-to-peak distances and resulting in larger step lengths. To account for potential missed steps, any step lengths exceeding 1 m or step times exceeding 3 s are excluded as outliers. Subsequently, if the linear track segment has a minimum of two measured step lengths, the average of these step lengths is calculated and considered as the average step length for the linear line segment L_i^k .

5. Experiment Setup

The study included individuals aged 60 years and older who met the following inclusion criteria: (1) frailty, indicated by a score of 3 or more on the FRAIL Scale, (2) lived alone, (3) had a home WiFi connection, and (4) had access to a smartphone or tablet for device setup. Exclusion criteria encompassed individuals who required a wheelchair for indoor mobility, needed prolonged sitting due to a medical condition, or lacked independent mobility. Participants with travel plans or commitments missing more than 30% of the study period were excluded. Participants were recruited from regional specialized geriatric clinics, community groups, and newspaper advertisements. This study was approved by Hamilton Integrated Research Ethics Board (HIREB Project# 15237) and was performed in accordance with the Declaration of Helsinki. Written informed consent was obtained from all participants.

Participants' demographic information (Table 2) was collected regarding age, sex, and education. Physical performance was assessed with the Short Physical Performance Battery (SPPB) [33]. An SPPB score of <9 points indicates poor physical performance and is predictive of hospitalization and mortality [34]. The Falls Efficacy Scale International (FES-I) is a standardized questionnaire that assesses concerns about falling within 16 physical and social activities at home and the community. FES-I items are rated on a four-point scale (1 (not at all concerned) to 4 (very concerned)), and total scores range from 16–64. FES-I total scores can be further classified based on the severity of the fear of falling with clinical cutoff points of no to low (score = 16–19) and moderate to high (score = 20–64) concern about falling [35]. Cognition was assessed with the Montreal Cognitive Assessment (MoCA) [36]. Total MoCA scores range from 0–30, and a score >26 points is considered normal cognitive function [36].

Table 2. Demographics of the participants. M—mean, SD—standard deviation, SPPB—Short Physical Performance Battery, FES—Fall Efficacy Scale, and MoCA—Montreal Cognitive Assessment.

Demographics	All Participants (N = 35)
Age, M (SD)	75.49 (6.56)
Age, Range	60 to 89
Sex, % female	30/35 (85.71%)
Education, n more than high school	23/35 (65.71%)
Living arrangement, n lives alone	35/35 (100%)
Physical function, SPPB total score, M (SD)	8.53 (2.74)
Physical function, n SPPB < 9	12/34 (35.29%)
Fear of falling, FES-I total score, M (SD)	24.97 (6.62)
Fear of falling, n FES-I moderate to high severity	26/34 (76.47%)
Cognition, MoCA total score, M (SD)	23.38 (3.64)
Cognition, n MoCA total score < 25	20/34 (58.82%)

5.1. Clinic Setup

Using the InCIANTI protocol [37], participants walked along the 4 m path during normal [control] and adaptive locomotion experimental conditions (walking while talking [dual task], reciting animal names from a given letter; obstacle crossing of two 4.5-inch-high obstacles; narrow walking along a 25 cm wide path; fast walking). Each of the five experimental conditions was conducted twice in a randomized order except for the fast walking trials, which were consistently performed last in each experimental block to avoid any influence on the speed of the preceding trials. Two blocks of walks were conducted within a participant session separated by approximately 30 min for intra-session reliability testing.

Participants commenced their walks at the beginning of the Zeno Walkway, proceeded to the end, and then came to a stop. Notably, unlike existing works [18,21–23], this approach encompasses the acceleration and deceleration effects associated with walking. This

methodology aligns with testing in home environments, as the limited space within homes makes it unfeasible to omit the acceleration and deceleration segments of the walks.

As shown in Table 3, of the 700 walks (35 participants \times 2 blocks \times 2 repetition \times 5 types of walks), 47 walks (across 6 participants) were not collected because the participants was too frail to complete the walks. A further 28 walks (across four participants) were not collected due to technical issues. The remaining 625 walks were collected with the Chirp sensor and the Zeno Walkway. The collected step lengths have a robust variation with a mean of 57 cm (12 cm), as shown in Figure 9.

Table 3. Of the 700 walks (35 participant \times 20 walks), data are missed due to technical difficulties and participants unable to complete the walks due to frailty.

	Control	Fast	Narrow	Obstacle	Dual Task	All
Tech. Difficulty	6	4	6	5	7	28 (4.0%)
Unable	1	4	17	24	1	47 (6.7%)
Collected Walks	133	132	117	111	132	625 (89.3%)

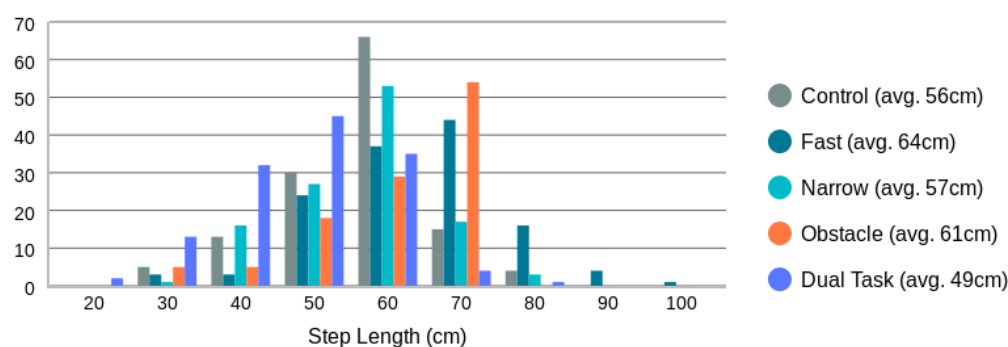


Figure 9. Ground truth step length distribution as measured by the Zeno Walkway Gait Analysis System. Overall average step length is 57 cm (12 cm).

5.2. Home

Participants installed the devices in their living room, bedroom, and kitchen for a two-week duration. Out of the 35 participants, 21 successfully set up the devices in their homes. Among these 21 participants, 3 have data for only one week, 1 participant has data for 10 days, and the remaining 17 have data for the full two weeks.

All participants reside alone. To ensure that the in-home evaluation of step length pertains solely to the participant, step length is reported only when a single person is being tracked within the home. Some participants have small pets, such as cats, which are excluded from tracking based on their size.

6. Algorithm Parameters

In-home track selection for step length measurement is dependent on three parameters: RDP threshold ϵ (Section 4.4.2), length of linear track segment D (12), and orientation threshold γ (12). Both ϵ and γ are set empirically as $\epsilon = 0.5$ m and $\gamma = 15^\circ$. Minimum length of track D must be selected to ensure at least two step lengths are present within the linear track segment (Section 4.5.2). Per [38], the average male step length for a walking speed of 1.6 m/s is 0.84 m. This requires a track length of at least 1.7 m for two steps. Based on this upper bound, D is set as $D = 2$ m.

The torso location cutoff, as defined in (16), must be defined based on known radar configuration. Participants were given instructions to set up the radar approximately at a height of 121 cm. Based on that, Z_{torso} is conservatively set as $Z_{torso} = 0.25$ m. This assumes that the torso radar points are within 0.25 m below to 0.25 m above the radar. This is empirically set based on the male average torso length of 46 cm to 52 cm.

Finally, the minimum peak-to-peak time R (Section 4.5.2) is set as small as possible. Given 10 FPS radar data and a center-surrounded non-maximum suppression window of 0.4 s (Section 4.5.2), the lower bound on R is $R > 0.4/2 = 0.2$ s. Based on this, the minimum peak-to-peak time is set as $R = 0.3$ s.

7. In-Clinic Step Length Evaluation

The study gathered data from 625 walks conducted in a clinic, with step length measurements simultaneously obtained from both the Chirp sensor and Zeno Walkway. This dataset serves as the basis for several evaluations. Firstly, an analysis of step length detection rate is conducted using the proposed method. Secondly, the concurrent validity of the proposed method is assessed against the gold-standard measurement obtained from the Zeno Walkway. Finally, a comparison of the proposed method with existing methods is undertaken.

7.1. Step Length Detection Rate

Over the 4 m walk, it is required to detect at least two step length measurements (i.e., three consecutive torso speed peaks) to generate an average step length measurement for the walk (refer to Section 4.5.2). Consequently, there are instances where the proposed method does not provide a step length measurement. Out of the 625 walks, the proposed method successfully detected step length in 599 walks, yielding a detection rate of 96%. The distribution of missed walk types is detailed in Table 4.

Table 4. Step length detection rates for the proposed approach on the 625 walks.

	Control	Fast	Narrow	Obstacle	Dual Task	All
Alg. Missed	2	18	6	0	0	26/625 (4.2%)
Alg. Detected	131	114	111	111	132	599/625 (95.8%)

As indicated in Table 4, the majority of missed step length measurements are associated with fast walks. This can be attributed primarily to the set minimum peak-to-peak time threshold of $R = 0.3$ s. The distribution of detected step length peak-to-peak times (i.e., step times) is illustrated in Figure 10. Notably, the distribution of step times for fast walks crosses the $R = 0.3$ s threshold. Consequently, the peak-to-peak measure for fast walks becomes undetectable in certain cases. To enable step length measurement at higher walking speeds, generating radar point clouds at a higher frame rate than 10 FPS and lowering the minimum peak-to-peak distance threshold from $R = 0.3$ s is necessary.

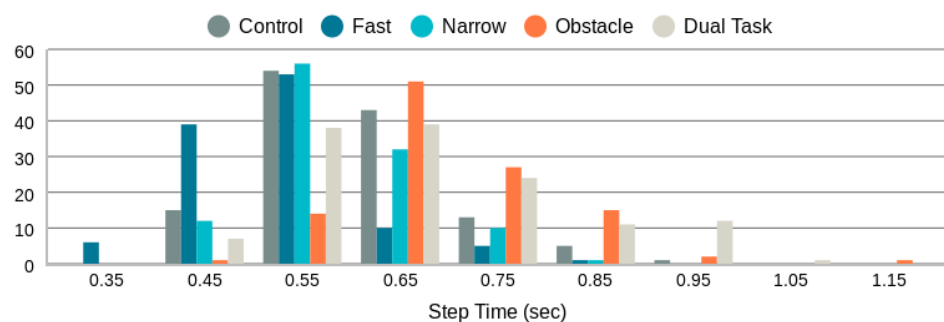


Figure 10. Distribution of step times as measured by torso speed peak-to-peak times.

In the context of in-home monitoring, there is no need for adjustments to the radar frame rate and peak-to-peak distance threshold. The step length measured at home typically appears smaller than what is observed in the clinic, as discussed in Section 8.2.

7.2. Concurrent Validity

Figure 11 displays all step length measurements obtained through the proposed radar-based method in comparison to those from the Zeno Walkway. Concurrent validity is evaluated by considering the absolute difference between Zeno Walkway step length measurements and those obtained using the proposed radar-based method. The analysis involves a total of 599 walks, where the proposed algorithm reported a step length. To address variations in individuals' step lengths (ranging from 26 cm to 97 cm, as illustrated in Figure 9), step length errors are further expressed as a percentage of the Zeno Walkway step length measurement. The comprehensive step length errors, along with a breakdown by different walk types, are presented in Table 5 and Figure 12.

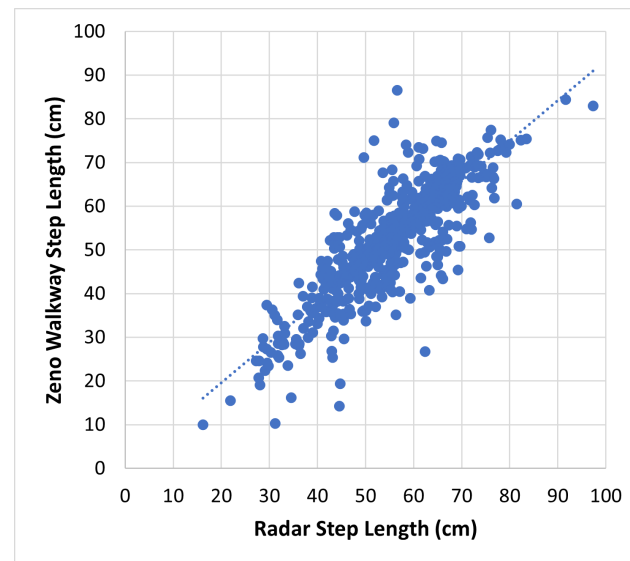
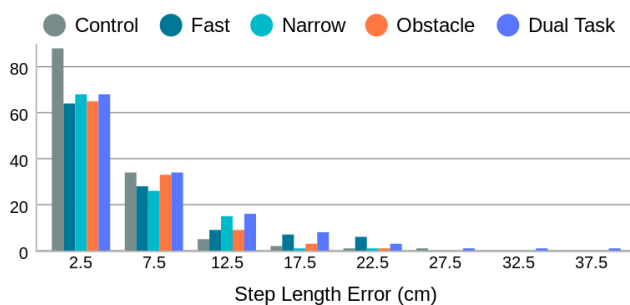
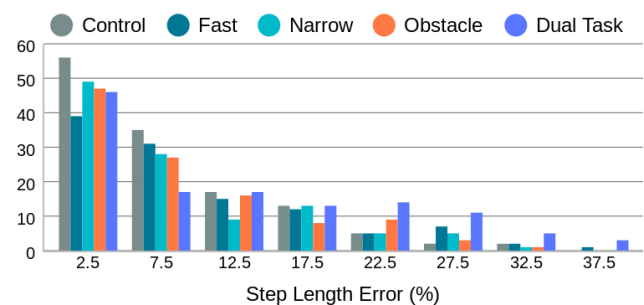


Figure 11. Proposed radar-based step length measurement vs. Zeno Walkway. Data include all 599 walks (4 m each) by 35 frail older adults.

In the control walk (i.e., normal walking speed), the average error is 4.5 cm, which, on average, is less than 10% of the true step length. Both narrow walkway walks and obstacle walks exhibit comparable absolute and relative errors. Fast walks and dual-task walks share the same absolute average error of 6.5 cm. However, the relative error for the dual task is 4% higher. This discrepancy arises from the fact that dual-task walks have shorter step lengths (refer to Figure 9) compared to fast walks. This underscores the significance of considering both absolute and relative step length errors in the assessment of step length measurement methods.



(a) Error distribution in cm.



(b) Error distribution % of step length.

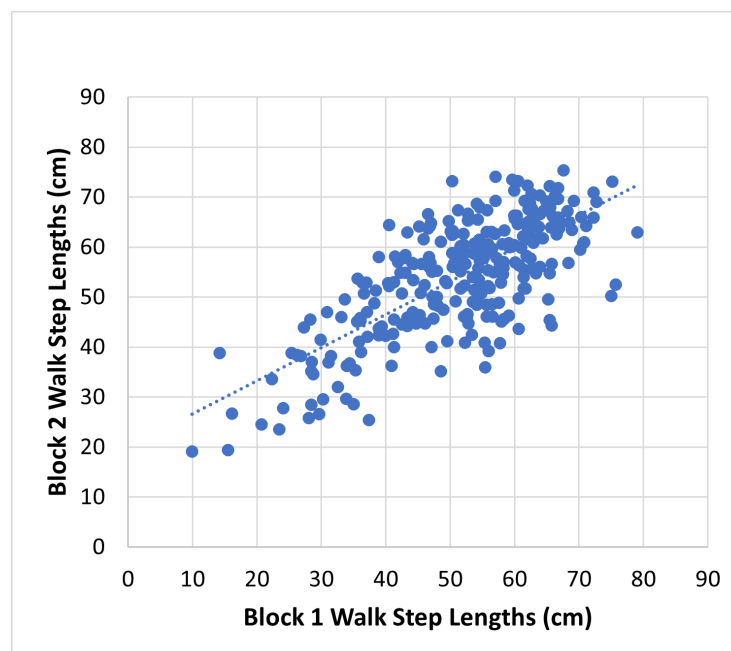
Figure 12. Step length error distribution by walk type in cm and as a percentage of the true step length measured by Zeno Walkway.

Table 5. Average (standard deviation) error in step length in cm and percentage of Zeno Walkway step length (%).

	Control	Fast	Narrow	Obstacle	Dual Task	All
cm	4.5 (4.3)	6.5 (5.9)	5.0 (4.3)	5.0 (4.4)	6.5 (6.4)	5.5 (5.2)
%	8.3 (8.0)	10.4 (9.3)	9.3 (9.2)	8.5 (7.4)	14.3 (13.4)	10.2 (10.1)

7.3. Intra-Session Reliability

To evaluate the reliability of the proposed method, we conducted an intra-session test–retest reliability analysis by comparing walks from block one to those in block two. The participants underwent an equivalent number and type of walks in both blocks to ensure consistency in measured step length. The reliability assessment is conducted using a two-way random effect, absolute agreement, and the multiple raters/measurement intra-class correlation (ICC) measure [39]. The measured step length between blocks is depicted in Figure 13, revealing $ICC(2,k) = 0.83$ (95% confidence interval (CI) 0.77 to 0.87). This indicates a strong level of reliability for the proposed approach in intra-session assessments within a clinical setting.

**Figure 13.** Intra-session reliability. Block 1 to block 2 step lengths measured in the clinic. $ICC(2,k) = 0.83$ (95% CI 0.77 to 0.87).

7.4. Comparison to Existing Methods

Although a direct comparison to existing radar-based step length measurement methods is not feasible, Table 6 provides a comparison based on the reported magnitude of error. The comparison utilizes the average from 131 control (normal) walks by frail older adults.

The errors reported in this study are two to four times larger in magnitude when compared to existing reported figures. However, it is crucial to acknowledge the specific focus of this work on step length measurement for frail older adults. Unlike healthy subjects with a consistent gait cycle, frail older adults exhibit variability due to factors such as health conditions. This is underscored by instances where some participants were unable to complete all 20 walks due to frailty reasons. Additionally, the distance traveled is shorter, and the walks include acceleration and deceleration components, factors expected in a home setting but not accounted for in previous works.

Table 6. Comparison to existing methods for normal walking in a controlled setting.

Method	Avg. Error (cm)	Total No. of Walks	No. of Participants	Distance (m)	Type
[21]	1.1 (0.8)	3	3	4	Young Fit
[22]	2.3	4	4	25.2	Young Fit
[18]	2.6 (1.5)	5	5	56	Young Fit
[23]	2.2 (1.4)	100	10	10	Young Fit
Ours	4.5 (4.3)	131	35	4	Older Frail

8. In-Home Step Length Evaluation

The measurement of step length in the home exclusively relies on the proposed radar-based system, preventing the possibility of concurrent validity assessment. Nevertheless, following literature on in-home gait speed analysis [15], we address the reliability of in-home step length measurement using a week-over-week test-retest framework and establish validity by correlating it with in-clinic step length measurements.

8.1. Reliability

Reliability is assessed through the test-retest framework, measuring step length from week one to week two within each room of the homes. This evaluation gauges the consistency of the proposed approach for step length measurement over the two weeks, assuming no significant change in step length occurs for the participants during this period. This assumption is corroborated by an end-of-study survey where participants reported no adverse outcomes such as falls. Additionally, the use of two different devices to obtain step length in each room between week one and week two introduces a test of inter-device reliability within the test-retest framework.

Figure 14 illustrates the average week-over-week step length measurements by the proposed approach for each room. Out of the 21 participants who set up the devices in their homes, 18 collected data over two weeks, resulting in a total of 18 participants \times 3 rooms = 54 rooms. However, some rooms did not have suitable tracks for measuring step lengths each week. Consequently, data from only 35 rooms across the 18 participants with reported average step lengths for the two weeks are presented in Figure 14.

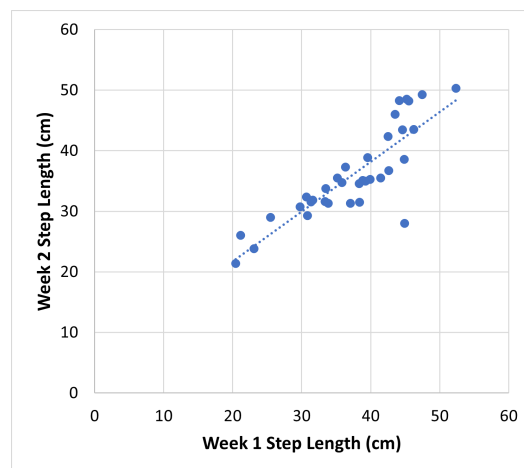


Figure 14. Average step length measurement, obtained by the proposed method, between week 1 and week 2 for each room. ICC(2,k) = 0.91 (95% CI 0.82 to 0.96), indicates excellent reliability.

Two-way random effect, absolute agreement, and multiple raters/measurement intra-class correlation (ICC) [39] are employed to quantify the absolute agreement between week 1 and week 2 step length measurements. Computed using the R software package v4.3.1, the ICC(2,k) = 0.91 (95% CI 0.82 to 0.96). This high ICC value indicates excellent reliability [39] for the proposed radar-based step length measurement in a home setting.

Figure 15 plots the test–retest reliability, as measured by ICC(2,k), against the step length averaging interval. The averaging interval goes from 2 days to 7 days in each week and as seen in Figure 15 and converges to an excellent reliability ($ICC(2,k) \geq 0.9$) for intervals of 5 days or greater.

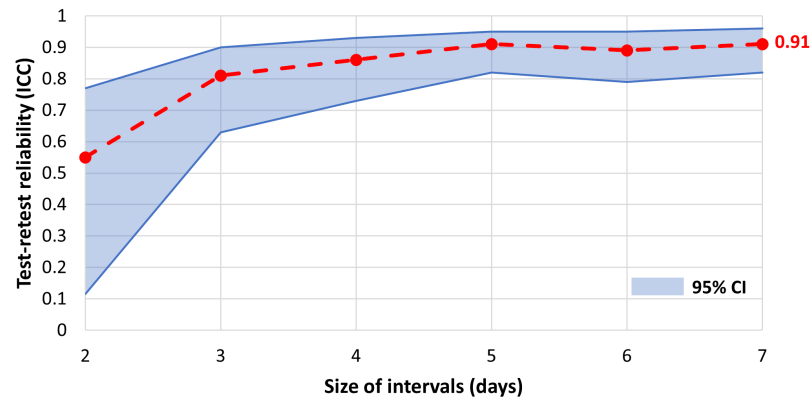


Figure 15. Test–retest reliability of in-home step length as a function of aggregation interval. Reliability is measured using inter-class correlation (ICC).

8.2. Validity

Validation of step length measurement in a home setting lacks ground truth. Nevertheless, the clinical assessment of each participant incorporates the measurement of step length during normal (control) walking. Although the step length measured during the clinical control walk may not precisely align with the average step length measured at home, a substantial correlation is anticipated. As a result, two-way random effects, consistency, and multiple raters/measurements inter class correlation (ICC) [39] are employed to evaluate the consistency between in-home measured step length and the in-clinic control walk step length.

In Figure 16, the control walk step length measurements in the clinic using the Zeno Walkway are compared to the average in-home step length measurements based on the proposed method for all 21 participants with in-home data. Computed using R v4.3.1, $ICC(3,k) = 0.81$ (95% CI 0.53 to 0.92), giving good consistency between the in-home and in-clinic measurements [39]. This affirms the validity of the proposed in-home step length measurement.

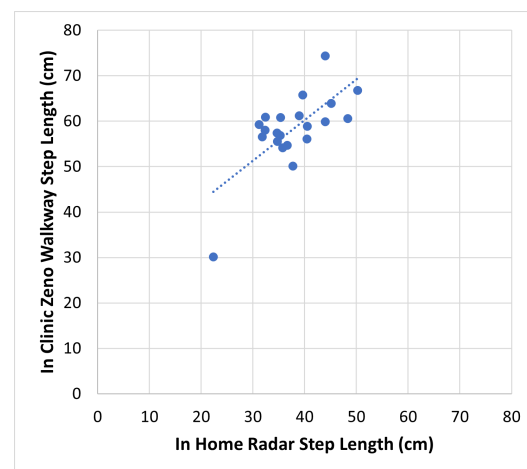


Figure 16. In-home average radar step length compared to in-clinic average control (normal walk) step length measured by Zeno Walkway. $ICC(3,k) = 0.81$ (95% CI 0.53 to 0.92), indicates strong consistency.

While correlated with in-clinic measurement, the in-home measured step length tends to be smaller than the assessment conducted in the clinic. This phenomenon aligns with

findings from other studies on gait speed, where in-home gait speed tends to be slower than that measured in a clinic setting [10].

A distinctive case worth highlighting is participant CHIRP024, who exhibited a significantly lower in-clinic step length measurement of 30 cm compared to other participants. Consistently, the in-home step length measurement for CHIRP024 is notably smaller than that of the other participants, as depicted in Figure 16. This observation further substantiates the credibility of the proposed measurement method.

Finally, Figure 17 illustrates the distribution of individual step lengths measured in the home, revealing distinct peaks corresponding to the averages identified in our previous analysis.

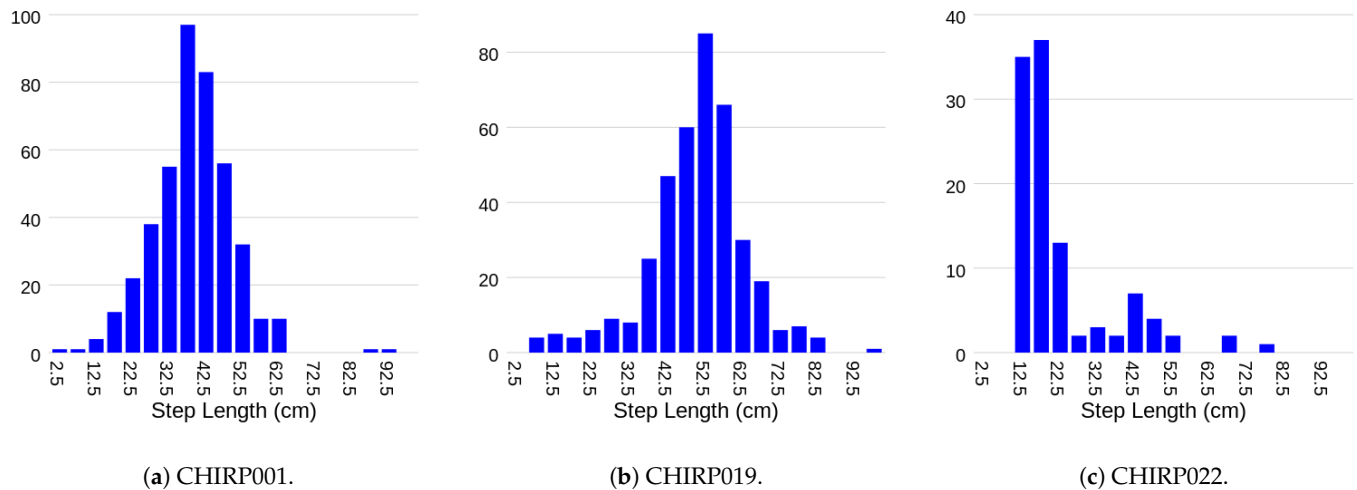


Figure 17. Distribution of all step lengths measured in the home over the full two-week data collection period.

9. In-Home Tracks

The proposed method relies on the assumption that, for the in-home setups selected by users, there are linear track segments that are at least $D = 2$ meters long and oriented within a $\gamma = 15^\circ$ angle of the radar's radial axis. In all 21 homes set up by participants, such tracks were identified, although their frequency varies significantly among homes. Figure 18 depicts the percentage of valid linear track segments, where step length can be measured. On average, valid track segments make up only a small percentage—17% (12%)—of the total observed tracks. Additionally, three of the homes have less than 5% valid tracks.

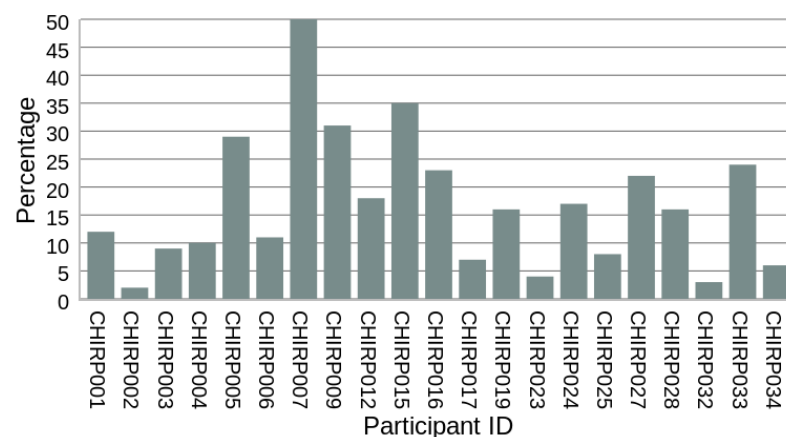


Figure 18. Percentage of valid linear track segments where step length can be measured. Valid linear track segments are linear track segments that are at least 2 m in length and within 15° of radar's radial axis direction.

The percentage of valid tracks is directly influenced by the home layout. For instance, consider CHIRP002, where only 2% of the tracks are suitable for step length measurement. The heatmap displaying all tracks in the home over a day is depicted in Figure 19a. It is evident that the long, frequently used pathways are nearly perpendicular to the radar's radial axis. In contrast, the heatmap of tracks in CHIRP007's home is more conducive to step length measurement (Figure 19b); with extended pathways aligned along the radar's radial axis, nearly 50% of the tracks are suitable for step length measurement.

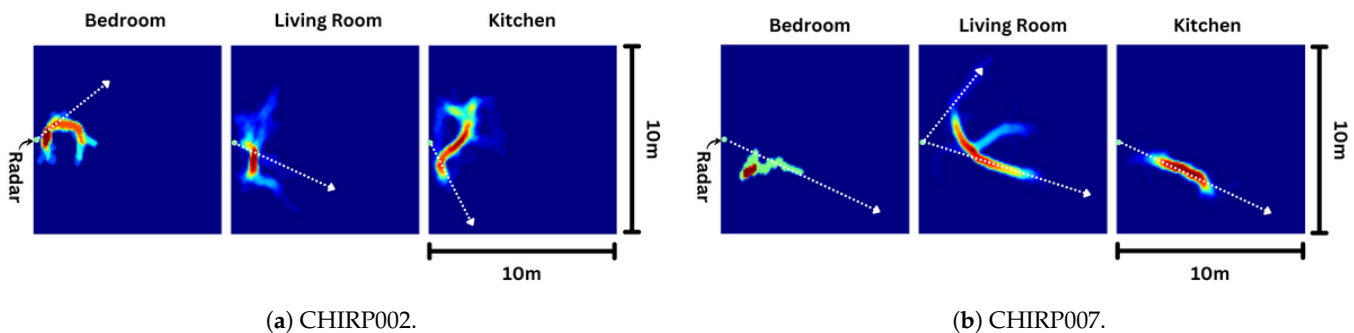


Figure 19. Heatmap of tracks in each room outlines the commonly used pathways in the home. CHIRP007's home has many commonly used pathways that lines up with radar's radial axis (illustrated in white dotted lines). CHIRP002's home's commonly used pathways do not line up with radar's radial axis.

10. Conclusions

This paper presents the first ever assessment of radar-based step length measurement for frail older adults in both clinical and home settings, confirming the feasibility of obtaining reliable and accurate step length measurements using radar sensors. Unlike existing publications, the proposed approach for step length measurement was evaluated using 35 frail older adults in a clinical environment and 21 frail older adults in a home setting. Clinic results demonstrate that radar-based step length measurement for frail older adults is within 4.5 cm of the gold-standard Zeno Walkway gait analysis system and exhibits strong intra-session reliability ($ICC(2,k) = 0.83$). In-home results indicates excellent week-over-week reliability ($ICC(2,k) = 0.91$) and a strong consistency ($ICC(3,k) = 0.81$) between in-home and in-clinic step length measurements. Both in-clinic and in-home results with frail older adults validates the real-time in-home step length measurement.

Having established the validity of the proposed radar-based step length measurement for frail older adults in a clinical setting, it becomes plausible to apply existing step length cutoffs [5] to anticipate adverse clinical events. Nevertheless, our findings indicate that while in-home step length is consistent with in-clinic measurements, it does not exhibit a one-to-one relationship. Specifically, in-home step length measurements tend to be smaller than those in a clinic setting. Consequently, the direct application of established step length cutoffs derived from clinical testing [5] may not seamlessly translate to in-home step length measurement. Instead, recognizing the high week-over-week reliability of the presented approach in measuring step length in the home, changes in step length in the home can be monitored for health risk assessment, as previously explored in [40].

Author Contributions: Conceptualization, P.S. and A.W.; methodology, P.S., A.W. and P.H.; formal analysis, P.S.; investigation, P.H., G.I. and A.P.; resources, J.A. and A.R.; writing—original draft preparation, P.S.; writing—review and editing, P.S., A.W., P.H., G.I., J.A., A.R., A.W.L. and A.P.; visualization, P.S.; funding acquisition, A.W.L., G.I. and A.P. All authors have read and agreed to the published version of the manuscript.

Funding: This research was funded by the Southern Ontario Pharmaceutical & Health Innovation Ecosystem (SOPHIE).

Institutional Review Board Statement: The study was conducted in accordance with the Declaration of Helsinki and approved by the Hamilton Integrated Research Ethics Board (HIREB) (Project# 15237, Protocol V6—26 June 2023).

Informed Consent Statement: Informed consent was obtained from all subjects involved in the study.

Data Availability Statement: The data presented in this study are available on request from the corresponding author.

Conflicts of Interest: Author P.S. owns stocks in Chirp Inc., the manufacturer of the sensor used in this study. All other authors declare no conflicts of interest. The funders had no role in the design of the study; in the collection, analyses, or interpretation of data; in the writing of the manuscript; or in the decision to publish the results.

Abbreviations

The following abbreviations are used in this manuscript:

CFAR	Constant False Alarm Rate
CI	Confidence Interval
DBSCAN	Density-Based Spatial Clustering of Applications with Noise
FES	Falls Efficacy Scale
FPS	Frames Per Second
ICC	Intra-class Correlation Coefficient
lidar	Light Detection and Ranging
MoCA	Montreal Cognitive Assessment
MOCAP	Motion Capture
NMS	Non-Maximum-Suppression
No.	Number
RDP	Ramer–Douglas–Peucker
SD	Standard Deviation
SDK	Software Development Kit
SNR	Signal-to-Noise Ratio
SPPB	Short Physical Performance Battery

References

1. Brohman, M.; ME, G.; Dixon, J.; Whittaker, R.; Fallon, L.; Lajkosz, K. Community Paramedicine Remote Patient Monitoring (CPRPM): Benefits Evaluation & Lessons Learned, 2015/17. *Can. Health Infoway* **2018**. Available online: <https://www.infoway-inforoute.ca/en/component/edocman/3542-community-paramedicine-remote-patient-monitoring-cprpm-benefits-evaluation-lessons-learned/view-document?Itemid=103> (accessed on 15 November 2023).
2. Middleton, A.; Fritz, S.L.; Lusardi, M. Walking speed: The functional vital sign. *J. Aging Phys. Act.* **2015**, *23*, 314–322. [[CrossRef](#)] [[PubMed](#)]
3. Fritz, S.; Lusardi, M. White paper: “walking speed: The sixth vital sign”. *J. Geriatr. Phys. Ther.* **2009**, *32*, 2–5. [[CrossRef](#)]
4. Rodríguez-Molinero, A.; Herrero-Larrea, A.; Miñarro, A.; Narvaiza, L.; Gálvez-Barrón, C.; Gonzalo León, N.; Valldosera, E.; de Mingo, E.; Macho, O.; Aivar, D.; et al. The spatial parameters of gait and their association with falls, functional decline and death in older adults: A prospective study. *Sci. Rep.* **2019**, *9*, 8813. [[CrossRef](#)] [[PubMed](#)]
5. Bytyçi, I.; Henein, M.Y. Stride length predicts adverse clinical events in older adults: A systematic review and meta-analysis. *J. Clin. Med.* **2021**, *10*, 2670. [[CrossRef](#)] [[PubMed](#)]
6. Kwon, M.S.; Kwon, Y.R.; Park, Y.S.; Kim, J.W. Comparison of gait patterns in elderly fallers and non-fallers. *Technol. Health Care* **2018**, *26*, 427–436. [[CrossRef](#)] [[PubMed](#)]
7. Kraus, M.; Saller, M.M.; Baumbach, S.F.; Neuerburg, C.; Stumpf, U.C.; Böcker, W.; Keppler, A.M. Prediction of physical frailty in orthogeriatric patients using sensor insole-based gait analysis and machine learning algorithms: Cross-sectional study. *JMIR Med. Inform.* **2022**, *10*, e32724. [[CrossRef](#)] [[PubMed](#)]
8. Woo, J.; Ho, S.C.; Yu, A.L. Walking speed and stride length predicts 36 months dependency, mortality, and institutionalization in Chinese aged 70 and older. *J. Am. Geriatr. Soc.* **1999**, *47*, 1257–1260. [[CrossRef](#)]
9. Kimura, A.; Paredes, W.; Pai, R.; Farooq, H.; Buttar, R.S.; Custodio, M.; Munugoti, S.; Kotwani, S.; Randhawa, L.S.; Dalezman, S.; et al. Step length and fall risk in adults with chronic kidney disease: A pilot study. *BMC Nephrol.* **2022**, *23*, 74. [[CrossRef](#)]
10. Atrsaei, A.; Corrà, M.F.; Dadashi, F.; Vila-Chã, N.; Maia, L.; Mariani, B.; Maetzler, W.; Aminian, K. Gait speed in clinical and daily living assessments in Parkinson’s disease patients: Performance versus capacity. *NPJ Park. Dis.* **2021**, *7*, 24. [[CrossRef](#)]

11. Piau, A.; Mattek, N.; Crissey, R.; Beattie, Z.; Dodge, H.; Kaye, J. When will my patient fall? Sensor-based in-home walking speed identifies future falls in older adults. *J. Gerontol. Ser. A* **2020**, *75*, 968–973.
12. Friedrich, B.; Steen, E.E.; Hellmers, S.; Bauer, J.M.; Hein, A. Estimating the gait speed of older adults in smart home environments. *SN Comput. Sci.* **2022**, *3*, 128. [[CrossRef](#)]
13. Bethoux, F.; Varsanik, J.S.; Chevalier, T.W.; Halpern, E.F.; Stough, D.; Kimmel, Z.M. Walking speed measurement with an Ambient Measurement System (AMS) in patients with multiple sclerosis and walking impairment. *Gait Posture* **2018**, *61*, 393–397. [[CrossRef](#)].
14. Joddrell, P.; Potter, S.; de Witte, L.P.; Hawley, M.S. Continuous in-home walking speed monitoring in older people with a low-cost ambient sensor: Results of a feasibility study. *Technol. Disabil.* **2021**, *33*, 77–85. [[CrossRef](#)]
15. Liu, Y.; Zhang, G.; Tarolli, C.G.; Hristov, R.; Jensen-Roberts, S.; Waddell, E.M.; Myers, T.L.; Pawlik, M.E.; Soto, J.M.; Wilson, R.M.; et al. Monitoring gait at home with radio waves in Parkinson’s disease: A marker of severity, progression, and medication response. *Sci. Transl. Med.* **2022**, *14*, eadc9669. [[CrossRef](#)] [[PubMed](#)]
16. Yagi, K.; Sugiura, Y.; Hasegawa, K.; Saito, H. Gait Measurement at Home Using A Single RGB Camera. *Gait Posture* **2020**, *76*, 136–140. [[CrossRef](#)] [[PubMed](#)]
17. Botros, A.; Gyger, N.; Schütz, N.; Single, M.; Nef, T.; Gerber, S.M. Contactless gait assessment in home-like environments. *Sensors* **2021**, *21*, 6205. [[CrossRef](#)] [[PubMed](#)]
18. Abedi, H.; Boger, J.; Morita, P.P.; Wong, A.; Shaker, G. Hallway Gait Monitoring Using Novel Radar Signal Processing and Unsupervised Learning. *IEEE Sens. J.* **2022**, *22*, 15133–15145. [[CrossRef](#)]
19. Wang, D.; Park, J.; Kim, H.J.; Lee, K.; Cho, S.H. Noncontact Extraction of Biomechanical Parameters in Gait Analysis Using a Multi-Input and Multi-Output Radar Sensor. *IEEE Access* **2021**, *9*, 138496–138508. [[CrossRef](#)]
20. Seifert, A.K.; Grimmer, M.; Zoubir, A.M. Doppler Radar for the Extraction of Biomechanical Parameters in Gait Analysis. *IEEE J. Biomed. Health Inform.* **2021**, *25*, 547–558. [[CrossRef](#)]
21. Veld, R. Human Gait Model Individualized by Low Cost Radar Measurements. Master’s Thesis, University of Twente, Enschede, The Netherlands, 2023.
22. Abedi, H.; Boger, J.; Morita, P.P.; Wong, A.; Shaker, G. Hallway Gait Monitoring System Using an In-Package Integrated Dielectric Lens Paired with a mm-Wave Radar. *Sensors* **2023**, *23*, 71. [[CrossRef](#)] [[PubMed](#)]
23. Saho, K.; Shioiri, K.; Kudo, S.; Fujimoto, M. Estimation of Gait Parameters From Trunk Movement Measured by Doppler Radar. *IEEE J. Electromagn. RF Microw. Med. Biol.* **2022**, *6*, 461–469. [[CrossRef](#)]
24. Winter, D. *The Biomechanics and Motor Control of Human Gait*; University of Waterloo Press: Waterloo, ON, Canada, 1987.
25. Sherratt, F.; Plummer, A.; Iravani, P. Understanding LSTM Network Behaviour of IMU-Based Locomotion Mode Recognition for Applications in Prostheses and Wearables. *Sensors* **2021**, *21*, 1264. [[CrossRef](#)] [[PubMed](#)]
26. Chirp Inc. Available online: <https://mychirp.com/> (accessed on 15 November 2023).
27. FCC ID 2A9Q4-CHIRP01T. Available online: <https://fccid.io/2A9Q4-CHIRP01T> (accessed on 15 November 2023).
28. Koyama, S.; Narita, E.; Shimizu, Y.; Suzuki, Y.; Shiina, T.; Taki, M.; Shinohara, N.; Miyakoshi, J. Effects of long-term exposure to 60 GHz millimeter-wavelength radiation on the genotoxicity and heat shock protein (HSP) expression of cells derived from human eye. *Int. J. Environ. Res. Public Health* **2016**, *13*, 802. [[CrossRef](#)] [[PubMed](#)]
29. Health Effects of mmWave Radiation. Available online: https://www.infineon.com/dgdl/Infineon-Health%20Effects%20of%20mmWave%20Radiation-PI-v01_01-EN.pdf?fileId=5546d46266a498f50166f1ada0520444 (accessed on 17 January 2024).
30. TI mmwave-sdk. Available online: <https://www.ti.com/tool/MMWAVE-SDK> (accessed on 15 November 2023).
31. Zhao, P.; Lu, C.X.; Wang, J.; Chen, C.; Wang, W.; Trigoni, N.; Markham, A. mID: Tracking and Identifying People with Millimeter Wave Radar. In Proceedings of the 2019 15th International Conference on Distributed Computing in Sensor Systems (DCOSS), Santorini, Greece, 29–31 May 2019; pp. 33–40. [[CrossRef](#)]
32. Hershberger, J.; Snoeyink, J. An O (n log n) implementation of the Douglas-Peucker algorithm for line simplification. In Proceedings of the Tenth Annual Symposium on Computational Geometry, Stony Brook, NY, USA, 6–8 June 1994; pp. 383–384.
33. Guralnik, J.M.; Simonsick, E.M.; Ferrucci, L.; Glynn, R.J.; Berkman, L.F.; Blazer, D.G.; Scherr, P.A.; Wallace, R.B. A Short Physical Performance Battery Assessing Lower Extremity Function: Association with Self-Reported Disability and Prediction of Mortality and Nursing Home Admission. *J. Gerontol.* **1994**, *49*, M85–M94. [[CrossRef](#)] [[PubMed](#)]
34. Negm, A.M.; Kennedy, C.C.; Pritchard, J.M.; Ioannidis, G.; Vastis, V.; Marr, S.; Patterson, C.; Misiaszek, B.; Woo, T.K.W.; Thabane, L.; et al. The Short Physical Performance Battery Is Associated with One-Year Emergency Department Visits and Hospitalization. *Can. J. Aging La Rev. Can. Du Vieil.* **2019**, *38*, 507–511. [[CrossRef](#)] [[PubMed](#)]
35. Yardley, L.; Beyer, N.; Hauer, K.; Kempen, G.; Piot-Ziegler, C.; Todd, C. Development and initial validation of the Falls Efficacy Scale-International (FES-I). *Age Ageing* **2005**, *34*, 614–619. [[CrossRef](#)] [[PubMed](#)]
36. Nasreddine, Z.S.; Phillips, N.A.; Bédirian, V.; Charbonneau, S.; Whitehead, V.; Collin, I.; Cummings, J.L.; Chertkow, H. The Montreal Cognitive Assessment, MoCA: A brief screening tool for mild cognitive impairment. *J. Am. Geriatr. Soc.* **2005**, *53*, 695–699. [[CrossRef](#)]
37. Deshpande, N.; Metter, E.J.; Guralnik, J.; Ferrucci, L. Can failure on adaptive locomotor tasks independently predict incident mobility disability? *Am. J. Phys. Med. Rehabil. Assoc. Acad. Physiatr.* **2013**, *92*, 704. [[CrossRef](#)]

38. Zarrugh, M.; Todd, F.; Ralston, H. Optimization of energy expenditure during level walking. *Eur. J. Appl. Physiol. Occup. Physiol.* **1974**, *33*, 293–306. [[CrossRef](#)]
39. Koo, T.K.; Li, M.Y. A guideline of selecting and reporting intraclass correlation coefficients for reliability research. *J. Chiropr. Med.* **2016**, *15*, 155–163. [[CrossRef](#)] [[PubMed](#)]
40. Brach, J.S.; Perera, S.; Studenski, S.; Katz, M.; Hall, C.; Verghese, J. Meaningful change in measures of gait variability in older adults. *Gait Posture* **2010**, *31*, 175–179. [[CrossRef](#)] [[PubMed](#)]

Disclaimer/Publisher’s Note: The statements, opinions and data contained in all publications are solely those of the individual author(s) and contributor(s) and not of MDPI and/or the editor(s). MDPI and/or the editor(s) disclaim responsibility for any injury to people or property resulting from any ideas, methods, instructions or products referred to in the content.